

Reactive Molecular Dynamics Calculation and Ignition Delay Test of the Mixture of an Additive and 2-Azido-*N,N*-dimethylethanamine with Dinitrogen Tetroxide

Jianshuo Zhao, Zhiyong Huang,* Guofeng Jin,* Minna Gao, and Huixin Zhu



Cite This: *ACS Omega* 2022, 7, 14527–14534



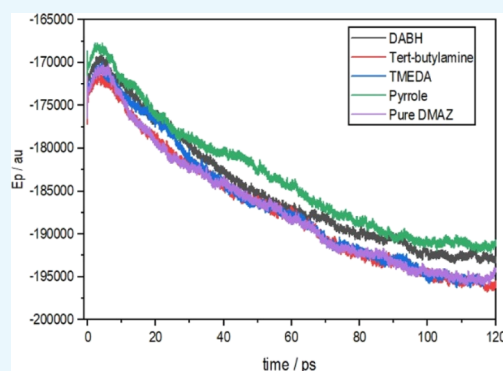
Read Online

ACCESS |

Metrics & More

Article Recommendations

ABSTRACT: In order to shorten the ignition delay of 2-azido-*N,N*-dimethylethanamine (DMAZ) and dinitrogen tetroxide (NTO), four amines [*tert*-butylamine, pyrrole, *N,N,N',N'*-tetramethyl ethylenediamine (TMEDA), and diethylenetriamine (DABH)] with a mass fraction of 5% were added to DMAZ, and the potential energy change and the product change during the reaction of the mixture of an additive and DMAZ with NTO were analyzed by Reactive molecular dynamics (ReaxFF MD) calculation. Then, the ignition delay of the mixture of the additive and DMAZ as well as pure DMAZ with NTO was measured by a drop experiment with a photoelectric sensor and high-speed camera. The results show that the addition of pyrrole greatly reduced the time to reach the maximum system energy and greatly increased the rate of HNO₂ formation. The dripping of the fuel was approximately a uniform linear motion, and the expression was $y = 43.13 + 7.16x$. The ignition delay time recorded by the camera was in good agreement with that of the optical signal. The measured ignition delay time for DMAZ with NTO was 261.5 ms. The mixture of pyrrole and DMAZ with NTO had the shortest ignition delay time of 100 ms, and the proportion of shortening the ignition delay time was the largest. The results of the droplet experiment were consistent with those of ReaxFF MD simulation, indicating that HNO₂ plays an important role in the ignition delay, that is, the formation rate of HNO₂ is positively correlated with the ignition delay.



1. INTRODUCTION

Azidamine fuels have the characteristics of high-density specific impulse, low freezing point, low toxicity, and no pollution. 2-Azido-*N,N*-dimethylethanamine, as a kind of non-carcinogenic spontaneous combustion fuel with a high specific impulse, has attracted much attention and is referred to as DMAZ.^{1–3} However, in a two-component system containing the dinitrogen tetroxide (NTO) oxidant, the ignition delay time of DMAZ and NTO was measured to be about 68 ms⁴ so the long ignition delay time cannot be widely applied. Therefore, it is necessary to study the mechanism of the ignition reaction between the fuel and oxidizer and analyze the factors affecting the ignition delay time.

The structure of a substance determines its properties and DMAZ has many conformations. McQuaid⁵ et al. characterized geometric parameters of 12 equilibrium conformations of DMAZ based on density functional theory and found that the most stable conformation is that with the central nitrogen atom of the azide group arranged above the lone pair electron of the amine nitrogen atom. Because this structure may inhibit proton transfer to the amine nitrogen atom, it can protect the lone pair electron of the amine nitrogen atom from the attack of nitric acid (NA) proton, which may be a key step to limit

the ignition reaction between DMAZ and NA. After obtaining the stable conformation of DMAZ, Zhang⁶ et al. studied the reaction of DMAZ with pure NA based on density functional theory and identified two important low-temperature reaction pathways: In the ignition reaction between DMAZ and NO₂, the first product is HNO₂, indicating that the formation of HNO₂ may play an important role in the ignition reaction.

For the reaction mechanism of spontaneous propellant ignition, the reaction path is mainly calculated by density functional theory, but there are many reaction paths and a large amount of calculation. Reactive molecular dynamics (ReaxFF MD) can calculate the dynamic evolution of the system driven by the reaction potential function, which does not require an artificially preset chemical reaction path. It has not only outstanding advantages in studying the microscopic chemical process in complex reaction systems but also great

Received: October 19, 2021

Accepted: March 25, 2022

Published: April 19, 2022



potential in studying the chemical reaction mechanism of complex systems.⁷

ReaxFF field is a reactive force field that describes bonding interactions between atoms on the basis of bond levels.⁸ Differently from the classical molecular force field, ReaxFF field optimizes and calculates the atomic charge dynamically in coulomb interaction calculation by adopting the electro-negativity balance method at each kinetic time step⁹ so that the ReaxFF field can better describe the polarization of atoms in the reaction system.^{10–12} The ReaxFF field divides atomic types by elements, such as C/H/O hydrocarbon systems, C/H/O/N energetic material systems, and metal oxide systems, to achieve portability and universality in describing different phase states. The training set data used for parameter fitting of the ReaxFF field comes from quantum mechanical calculation and experimental data, so ReaxFF MD calculation has been widely used to reveal the microscopic details of pyrolysis,¹³ oxidation,¹⁴ catalysis,¹⁵ combustion,¹⁶ and many other complex reactions.

Shortening the ignition delay time of spontaneous combustion is an important factor for engine design and propellant research and development. Compounding is an advanced method to shorten the ignition delay time. Nusca¹⁷ et al. developed a complete and detailed chemical kinetic mechanism of the *N,N,N',N'*-tetramethyl ethylenediamine (TMEDA)-DMAZ/red fuming NA (RFNA) system based on computational chemistry techniques. When CHEMKIN was used to simulate the behavior of the TMEDA-DMAZ/RFNA system, the mechanism predicted a shorter ignition delay than for TMEDA/RFNA and DMAZ/RFNA. William H.¹⁸ studied the system using IRFNA as the oxidant. The ignition delay time of MMH measured at 30 °C was about 3–15 ms. The ignition delay of TMEDA was about 14 ms. The ignition delay of DMAZ was approximately 26 ms. When 33.3% DMAZ and 66.7% TMEDA were added into the fuel mixture, the ignition delay could be adjusted to 9 ms.¹⁹ Pakdehi²⁰ carried out a dripping experiment under environmental pressure and temperature with the aid of a high-speed camera to add several amines as compounding agents to DMAZ and measured the ignition delay time between them and white fuming NA (WFNA). The results showed that adding pyrrole, *tert*-butylamine, and octylamine to DMAZ significantly shortened the ignition delay of DMAZ and WFNA.

Based on the calculation by ReaxFF MD and the independent dropping experiment, this paper studied the factors affecting the ignition delay of DMAZ and NTO through the comparative analysis of theory and experiment to provide reference for the analysis of ignition delay time, understanding of the spontaneous combustion process of bipropellants, synthesis of green propellants, and design of new propellants.

2. THEORETICAL AND EXPERIMENTAL METHODS

2.1. Theoretical Method. Based on the ReaxFF MD method, the reaction process of NTO with pure DMAZ and the mixture of DMAZ and four amines (*tert*-butylamine, pyrrole, TMEDA, and DABH) was calculated at 2500 K. These molecules are randomly inserted into the simulation chamber and subjected to energy minimization. After energy minimization, steps of 0.4 fs are performed under the NVT ensemble, and the total length of the simulation is 120 ps. The cumulative effect of iteration error was eliminated by adjusting the atomic velocity at each step. The temperature was

controlled by the Berendsen method, the coupling constant was 0.1 ps, and the bond level truncation radius was 0.3. The size of the bond level truncation radius was used to determine whether the atoms are connected. According to the calculation at 2500 K, the reaction can be completed in a few hundred picoseconds, and the reaction potential energy change and the change of the product were obtained. The reaction process was calculated by canonical ensemble (NVT) and completed by the LAMMPS program package.²¹ Because the research system in this paper contains C, H, O, and N elements, the ReaxFF parameters²² for C/H/O/N compounds were used in our simulations.

2.2. Experimental Methods. **2.2.1. Experimental Materials and Instruments.** Experimental materials are shown in Table 1.

Table 1. Experimental Materials

name	specification (%)	density/g·cm ⁻³	Source
<i>tert</i> -butylamine	99	0.696	Shanghai Titan Technology Co., Ltd.
pyrrole	99	0.967	Shanghai Titan Technology Co., Ltd.
TMEDA	99	0.775	Shanghai Titan Technology Co., Ltd.
DABH	99	0.955	Shanghai Titan Technology Co., Ltd.

Experimental materials are rated reagent grade (RG) and can be used as standard chemicals for reagents, so they are of high purity. To ensure stability of the materials, DMAZ, *tert*-butylamine, pyrrole, TMEDA, and DABH were stored at 5 °C and NTO was stored at -10 °C. Fuel and oxidizers needed to be stored separately because of their spontaneous combustion.

The experimental instruments are shown in Table 2.

Table 2. Experimental Instruments

name	specification	Source
microsyringe	100 μL	Ningbo Zhenhai Sanai Instrument Factory
oscillograph	DS1104Z-S Plus	Puyuan Jingdian Technology Co., Ltd.
voltage-stabilized source	KORAD/KA3005D	Shenzhen Keriyuan Technology Co., Ltd.
grating sensor	NZD-B50	Shenzhen Xinmeitai Technology Co., Ltd.
optical sensor	SENSORIK FSP30	Beijing Konrad Electromechanical Technology Co., Ltd.
high-speed camera	YVSION/OSG030-790UM	Shenzhen Yingshi Technology Co., Ltd.

2.2.2. Experimental Principles. The photoelectric recording principle: adjust the voltage regulator so that it outputs a stable voltage and current. The power supply is connected by a wire to three sensors, two grating sensors (grating 1 at the top, grating 2 at the bottom), and an optical signal sensor, which are respectively connected to the three channels of the digital oscilloscope. The contact probes of three sensors are used to collect and record the signals: two grating sensors are used to record the signal channel 1 (CH1) and channel 2 (CH2) passing through the droplet, and an optical signal sensor was used to sense the optical signal channel 3 (CH3) generated at the moment of ignition. The time difference between the fuel

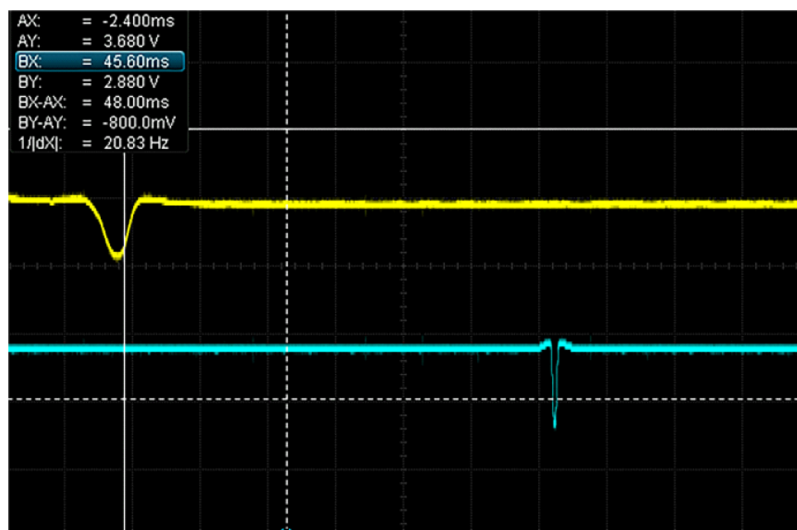


Figure 1. Peak display of signal CH1 and signal CH2.

droplet passing through the two grating sensors is denoted as t_1 , and the time difference between the droplet passing through grating 1 and the optical signal sensor is denoted as t_2 . Then, the ignition delay time is

$$t_{\text{photoelectric}} = t_2 - t_1 \quad (1)$$

The camera recording principle: a high-speed camera is used to take pictures of the ignition reaction process and then export pictures for analysis. The time when the fuel contacts the oxidizer is marked as t_3 and the time until an obvious flame appears as t_4 . Then, the ignition delay time is

$$t_{\text{camera}} = t_4 - t_3 \quad (2)$$

2.2.3. Experimental Design. The photoelectric instrument: adjust the voltage regulator power supply so that the output voltage is 6.7 V and the current is 0.1 A. Grating 1 and grating 2 are connected, and the oscilloscope is connected so that signals CH1 and CH2 are stable. Adjust the voltage signal value of each cell of the two grating sensors to 200 mV, and set the time interval to 20 ms so that the droplet will display an obvious peak value when it drops as shown in Figure 1.

Adjust the voltage signal value of each cell of the optical signal sensor to 2 V and set the time interval to 50 ms to facilitate signal acquisition. The signals CH1 and CH3 are displayed, and the results are shown in Figure 2.

The high-speed camera: Place the high-speed camera on the tripod, adjust the appropriate angle and height so that the high-speed camera can be aligned with the bottom of the beaker, and adjust the aperture and focus. After the computer is

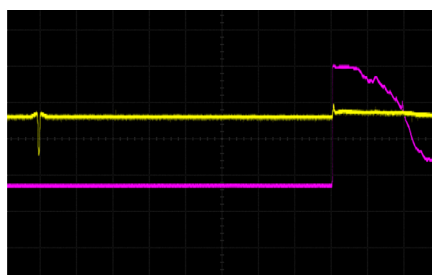


Figure 2. Peak display of signal CH1 and signal CH3.

connected, the ignition process between fuel and NTO is clearly seen as shown in Figure 3.



Figure 3. Ignition process of fuel and NTO: fuel contact with NTO liquid surface; white fog production; and ignition.

Resolution of high-speed cameras corresponds to the number of frames as shown in Table 3. As the ignition delay

Table 3. Corresponding Resolution and Frames/Second

resolution	frames/second
640 × 480	790
640 × 374	1000
640 × 238	1500
640 × 172	2000
640 × 104	3000
640 × 72	4000
640 × 32	6600

time is in the order of ms, and the definition of shooting is considered, 1000 frames are selected for high-speed camera shooting, and exposure time is set to 0.9 ms.

For the high-speed camera reading, there is an artificial observation error in the determination of the contact time and the ignition time of the droplet, but because the picture is 1000 frames per second, it has little influence on the determination of the ignition delay period.

One drop (about 10 μL) of the fuel is dripped with a 100 μL syringe located above the grating and 1.4 mL of oxidizer was placed in a 25 mL beaker. For the use of syringes, under the influence of experimental ambient temperature, the droplet size of syringes is affected, and the shaking of hands or improper operation methods also affects the droplet size. Therefore, in actual operation, external temperature and human factors should be strictly controlled to reduce the

error of experimental data. The basic framework of the dripping experiment is shown in Figure 4.

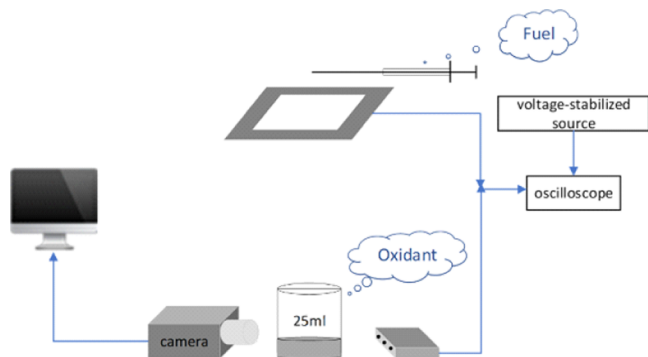


Figure 4. Basic framework of the dripping experiment.

As a green propellant, DMAZ is stable at room temperature and safe to operate. Oxidizer NTO is volatile at room temperature and produces a reddish-brown gas, which is dangerous to some extent. Therefore, the experiment in this paper was carried out in a laboratory with ventilation devices.

3. RESULTS AND DISCUSSION

3.1. ReaxFF MD Calculation of DMAZ with NTO. The simulated reaction between DMAZ and NTO took place in a $3.7 \text{ nm} \times 3.7 \text{ nm} \times 3.7 \text{ nm}$ box, and the density was set to $0.6 \text{ g}\cdot\text{cm}^{-3}$. The number of *tert*-butylamine, pyrrole, TMEDA, and DABH molecules in the DMAZ box was 5, 5, 3, and 3, respectively, to ensure that the mass fraction of the additive was 5%. The number of molecules of DMAZ and additives is shown in Table 4.

Table 4. Molecular Number of DMAZ and Additives

serial number	1	2	3	4	5
DMAZ	64	60	59	60	60
NTO	128	128	128	128	128
<i>tert</i> -butylamine	0	5	0	0	0
pyrrole	0	0	5	0	0
TMEDA	0	0	0	3	0
DABH	0	0	0	0	3

Molecules were inserted randomly into the box to better simulate the actual reaction process. The reaction of DMAZ and NTO with the addition of the compounding agent is accompanied by the change of energy, and the change of potential energy (E_p) is shown in Figure 5.

As the reaction progresses, the potential energy of the system first increases sharply and then decreases. In the simulated reaction between DMAZ and NTO, the potential energy reached the maximum at $t = 6.20 \text{ ps}$ and then decreased. The time to reach the maximum DMAZ energy after the addition of the additive was shortened as shown in Table 5.

DMAZ with different additives took different time to reach the maximum energy. The shortest time to reach the maximum value was 2.94 ps for pyrrole, for *tert*-butylamine 3.24 ps, DABH 3.89 ps, and TMEDA 4.27 ps. The results showed that DMAZ with additives absorbed energy faster, which was beneficial to triggering the reaction and achieving the purpose of rapid ignition.

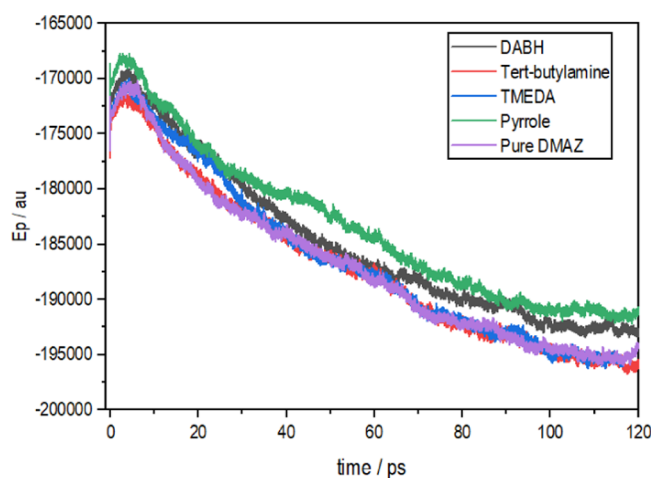


Figure 5. Potential energy changes in the reaction between pure DMAZ and DMAZ with a compounding agent and NTO.

Table 5. Time to Reach the Maximum Energy

additives	<i>tert</i> -butylamine	Pyrrole	TMEDA	DABH
time/ps	3.24	2.94	4.27	3.89

The reaction between DMAZ and NTO is accompanied by breaking of old chemical bonds and formation of new chemical bonds. At $T = 2500 \text{ K}$, the evolution of chemical species in the kinetics of pure DMAZ as well as the mixture of the additive and DMAZ with NTO was obtained, and the generation of HNO_2 played an important role in the ignition reaction. Therefore, the changes of HNO_2 species were mainly analyzed as shown in Figure 6.

The letter N on the Y axis represents the number of molecules, indicating the change of the amount of intermediate HNO_2 generated with the change of time during the simulated reaction. Figure 7 shows the change of HNO_2 molecule number after the addition of an amine complex in DMAZ.

The molecule number of HNO_2 produced by DMAZ with a compounding agent reached the maximum in the period of 5–15 ps. Pure DMAZ reached the maximum value at 13.5 ps, and the number was 21. DMAZ with *tert*-butylamine, pyrrole, TMEDA, and DABH reached maximum values at 14.6, 6.6, 11.0, and 8.9 ps, respectively, and the numbers were 25, 25, 26, and 32, respectively.

To better compare the generation rate of HNO_2 , the curve from the initial generation to the maximum molecule number of HNO_2 was fitted as shown in Table 6.

As can be seen from Table 6, the slope of the generation curve for pure DMAZ was 0.98, and that for DMAZ with *tert*-butylamine, pyrrole, TMEDA, and DABH was 3.26, 3.48, 2.04, and 1.11, respectively. After the addition of pyrrole, the formation rate of HNO_2 was greatly improved, and the correlation coefficient reached 0.94, indicating the reliability of the linear fitting data. Therefore, it can be predicted that adding pyrrole can accelerate the ignition reaction and shorten the ignition delay.

3.2. Determination of Ignition Delay Time in the Dripping Experiment. **3.2.1. Determination of Drop Time t_1 .** First, the relationship between drop time and drop height was measured, and the drop height between two photoelectric sensors was set to 3, 6, 9, 12, and 15 cm, and the drop time was measured. The data are shown in Table 7.

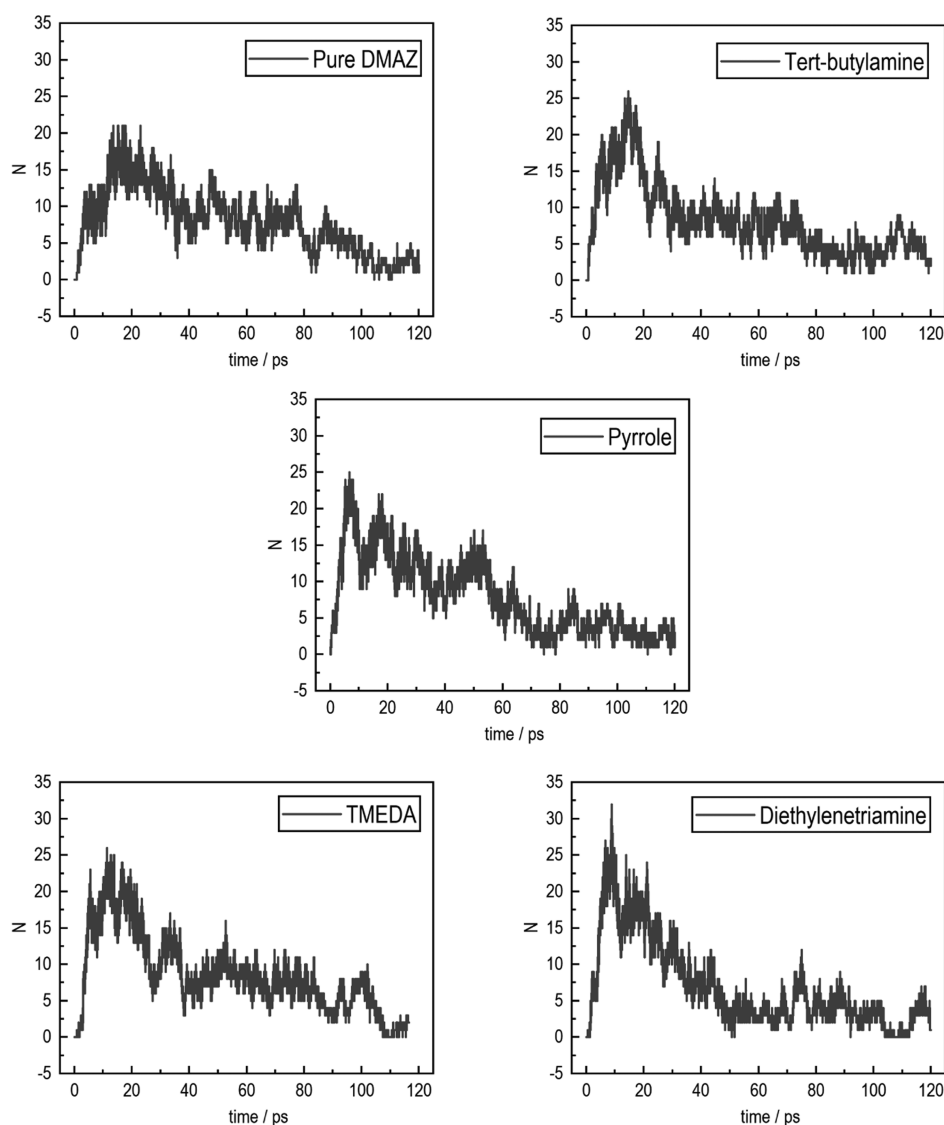


Figure 6. Changes of HNO_2 species in the reaction of pure DMAZ and the mixture of the additive and DMAZ with NTO.

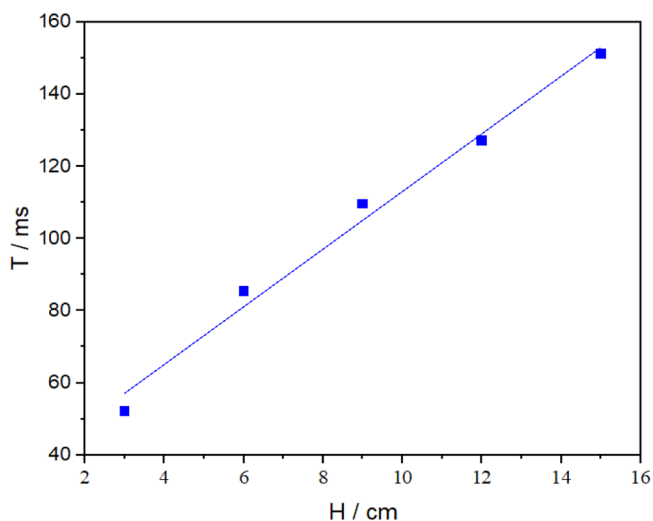


Figure 7. Relationship between drop time and drop height.

The average value of the six measurements was taken to draw a graph, and the result is shown in Figure 7.

It can be seen from Figure 7 that within a certain distance, the dropping process is approximately a uniform linear motion. By fitting the line, this expression was obtained: $y = 43.13 + 7.16x$. Fitting coefficient was 0.9981, intercept error was 3.44701, and the slope error was 0.31272. The drop height selected in the experiment was 10.5 cm, so the calculated time of droplet passing through grating 1 and grating 2 was 118 ms, that is, t_1 was 118 ms.

3.2.2. Ignition Delay of DMAZ and NTO. The length of ignition delay and the test conditions such as the mixing ratio of fuel and oxidant, temperature, and fuel and oxidant contact with a degree of atomization (degree of atomization is associated with the system pressure and sample viscosity) are closely related. The influence of temperature and material ratio was not considered in the test.

In the dripping experiment, a photoelectric signal and camera recording were used to calculate the ignition delay time $t_{\text{photoelectric}}$ and t_{camera} .

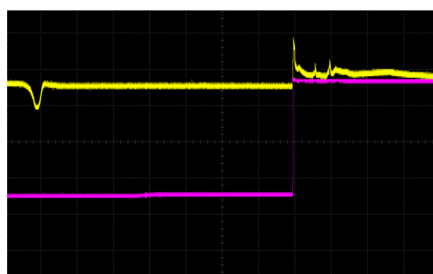
Optical signal reading: the time difference between the time when the droplet begins to pass through grating 1 and the optical signal sensor and the ignition time is denoted as t_2 as shown in Figure 8, which is $t_{\text{photoelectric}}$.

Table 6. Fitting Line of HNO₂ Formation Rate for Pure DMAZ and the Mixture of the Additive and DMAZ with NTO

additives	the linear expression of the fit	the slope error	intercept errors	correlation coefficient (R^2)
DMAZ	$y = 0.98x + 2.31$	0.00296	0.02444	0.73
<i>tert</i> -butylamine	$y = 1.11x + 5.50$	0.00358	0.03064	0.73
pyrrole	$y = 3.48x + 0.14$	0.0067	0.02538	0.94
TMEDA	$y = 2.04x + 0.50$	0.00604	0.03847	0.80
DABH	$y = 3.26x - 1.46$	0.00549	0.02807	0.94

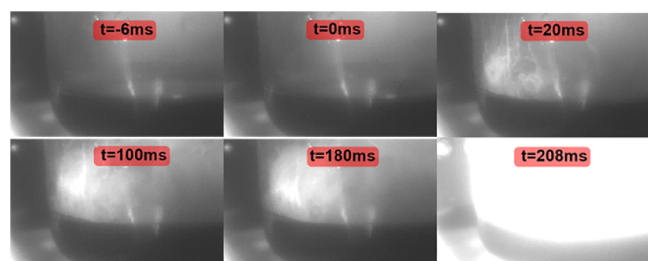
Table 7. Drop Time of DMAZ Droplet at 3, 6, 9, 12, and 15 cm

serial number	height/cm, drop time/ms				
	3	6	9	12	15
1	48.4	85.2	117.6	129.2	150.8
2	49.0	90.2	117.2	124.0	150.0
3	59.8	85.4	106.0	126.4	148.2
4	46.0	83.2	104.0	130.4	148.0
5	48.8	82.0	106.4	122.0	158.0
6	61.0	86.2	106.4	130.6	151.8

**Figure 8.** Signal of droplet initiation (yellow line) and the signal of ignition time (purple line).

It can be seen from Figure 8 that t_2 was 354 ms. It can be obtained from Section 3.2.1 that t_1 was 118 ms. Therefore, the measured $t_{\text{photoelectric}}$ was 236 ms, that is, the ignition delay time of DMAZ and NTO was 236 ms.

Camera reading: the process from droplet dropping to ignition was recorded, and the time from the contact between fuel and oxidizer was recorded as $t = 0$ ms, as shown in Figure 9.

**Figure 9.** DMAZ dripping into the NTO pool.

It can be obtained from Figure 9 that t_{camera} was 208 ms, that is, the ignition delay time of DMAZ and NTO was 208 ms.

The ignition experiment of DMAZ and NTO was carried out six times. By comparing the same experiment, it can be found that the values of reading by the camera and by the optical signal are in good agreement. These two methods have high accuracy and can be applied to the determination of basic ignition delay time. The value read by the camera had little

fluctuation, so the average result of reading by the camera was the ignition delay time, that is, the ignition delay time of DMAZ and NTO was 261.5 ms.

3.2.3. Effect of the Additive on Ignition Delay of DMAZ and NTO. DMAZ and NTO, as a kind of self-igniting two-component propellant, have a long ignition delay time. Therefore, for the wide application of DMAZ and NTO combination, it is necessary to explore the addition of additives to DMAZ to reduce the ignition delay of DMAZ and NTO. Amines have the characteristics of fuel, and some amines can directly react with NTO on fire. By adding amines, the influence on the ignition delay was analyzed, thus providing reference for the wide application of azidamine. According to the literature review, the additive ratio of 5% mass fraction does not affect the ratio of oxidizer to fuel, so the ratio of 5% mass fraction was selected in the experiment.

After the additive had been added to DMAZ, the DMAZ solution with *tert*-butylamine, pyrrole, and TMEDA was in a clear state, whereas the DMAZ solution with DABH was in a turbid state, which was analyzed to be related to the characteristics of high molecular weight and large molecular aggregation of DABH. After a period of time, all four solutions became clear.

With the help of a high-speed camera, the ignition delay time of the mixture of the additive and DMAZ with NTO was calculated. Three dripping experiments were conducted, and the average value of the ignition delay time was taken. The results are shown in Table 8.

Table 8. Shortening Ratio of DMAZ and NTO Ignition Delay by Additives

additives	<i>tert</i> -butylamine	pyrrole	TMEDA	DABH
ignition delay/ms	192.7	100.0	110.7	123.3
shortening ratio/%	26.3	61.8	57.7	52.8

As shown in Table 8, the addition of *tert*-butylamine, pyrrole, TMEDA, and DABH to DMAZ shortened the ignition delay of DMAZ and NTO. The results show that adding amines can shorten the ignition delay of DMAZ and NTO. With the addition of different amines, the proportion of DMAZ and NTO ignition delay was also different. DMAZ and NTO with pyrrole had the shortest ignition delay, with the shortening ratio of 61.8%. DMAZ and NTO with *tert*-butylamine had the longest ignition delay and the smallest shortening ratio (26.3%), which was consistent with the simulation results by ReaxFF MD.

4. CONCLUSIONS

Based on ReaxFF MD calculation and the droplet experiment, this paper studied the influence of adding four amines (*tert*-butylamine, pyrrole, TMEDA, and DABH) with 5% mass fraction to DMAZ in the ignition reaction between DMAZ and

NTO from the theoretical and experimental point of view and drew the following conclusions:

- (1) Based on ReaxFF MD calculation, the reaction time between DMAZ and NTO with added amines was shortened when the energy reached the maximum value. The shortest time to reach the maximum energy was 2.94 ps for pyrrole, for tert-butylamine it was 3.24 ps, DABH 3.89 ps, and TMEDA 4.27 ps. DMAZ with additives can absorb energy more quickly, which was conducive to triggering the reaction and achieving the purpose of rapid ignition. Meanwhile, the formation rate of HNO₂ increased. For a few HNO₂ molecules, pure DMAZ reached the maximum value at 13.5 ps, and the number was 21. DMAZ with tert-butylamine, pyrrole, TMEDA, and DABH reached the maximum value at 14.6, 6.6, 11.0, and 8.9 ps, respectively. The slope of the fitting curve of HNO₂ generation was 0.98 for pure DMAZ and NTO and for DMAZ with tert-butylamine, pyrrole, TMEDA, and DABH 3.26, 3.48, 2.04, and 1.11, respectively.
- (2) With the help of photoelectric sensors and a high-speed camera, the ignition delay of pure DMAZ and the mixture of the additive and DMAZ with NTO was measured. In a certain distance, the dropping process was approximately a uniform linear motion. The expression was obtained by fitting the line: $y = 43.13 + 7.16x$. The data obtained with the camera and optical signal were in good agreement. The results show that the two methods have high accuracy and can be applied to the determination of basic ignition delay time. The value read with the camera had little fluctuation, so the average result of reading with the camera was the ignition delay time, that is, the ignition delay time of DMAZ and NTO was 261.5 ms. DMAZ and NTO with pyrrole had the shortest ignition delay time (100 ms) and the largest reduction of ignition delay time (61.8%).
- (3) HNO₂ plays an important role in the ignition delay, that is, the generation rate of HNO₂ is positively correlated with the ignition delay. Based on ReaxFF MD simulation, the formation rate of HNO₂ greatly increased with the addition of pyrrole. In the dripping experiment, the mixture of pyrrole and DMAZ with NTO had the shortest ignition delay and the largest proportion of shortening the ignition delay. The dripping experiment agrees with ReaxFF MD calculation.


AUTHOR INFORMATION

Corresponding Authors

Zhiyong Huang – Xi'an Institute of High Technology, Xi'an 710000 Shaanxi Province, China; Email: john69@sina.com

Guofeng Jin – Xi'an Institute of High Technology, Xi'an 710000 Shaanxi Province, China; Email: douhao616@126.com

Authors

Jianshuo Zhao – Xi'an Institute of High Technology, Xi'an 710000 Shaanxi Province, China;  orcid.org/0000-0002-3629-5926

Minna Gao – Xi'an Institute of High Technology, Xi'an 710000 Shaanxi Province, China

Huixin Zhu – Xi'an Institute of High Technology, Xi'an 710000 Shaanxi Province, China

Complete contact information is available at:

<https://pubs.acs.org/10.1021/acsomega.1c05869>

Notes

The authors declare no competing financial interest.

REFERENCES

- (1) Mellor, B. A. Preliminary Technical Review of DMAZ: A Low-Toxicity Hypergolic Fuel. *Proceedings of 2nd International Conference on Green Propellants for Space Propulsion*; Cagliari: Sardinia, Italy, 2004.
- (2) Zhao, X.; Yanling, L. I.; Gao, Y. Current Status and Development Trend of Liquid Propellant. *The Eighth National Academic Conference on Chemical Propellants of Chinese Chemical Society, Qingdao, Shandong, China, Proceedings*, 2017; pp 141–151.
- (3) Reddy, G.; Song, J.; Mecchi, M. S.; Johnson, M. S. Genotoxicity assessment of two hypergolic energetic propellant compounds. *Mutat. Res.* **2010**, *700*, 26–31.
- (4) Hampton, K. K. R. C. S.; Smith, J. E., Jr. *Importance of Chemical Delay Time in Understanding Hypergolic Ignition Behaviors*, Reno, Nevada. AIAA 2003-1359, 2003.
- (5) McQuaid, M. J.; McNesby, K. L.; Rice, B. M.; Chabalowski, C. F. Density functional theory characterization of the structure and gas phase, mid-infrared absorption spectrum of 2-azido-N, N-dimethylethanamine (DMAZ). *J. Mol. Struct.: THEOCHEM* **2002**, *587*, 199–218.
- (6) Zhang, P.; Zhang, L.; Law, C. K. Density functional theory study of the reactions of 2-azido-N, N-dimethylethanamine with nitric acid and nitrogen dioxide. *Combust. Flame* **2015**, *162*, 237–248.
- (7) Renxing, C. *Molecular Dynamics Simulation of cl-20 Eutectic Thermal Decomposition of Panoramic Reaction Mechanism*; University of Chinese Academy of Sciences (Institute of Process Engineering, Cas), 2020.
- (8) Senftle, T. P.; Hong, S.; Islam, M. M.; Kylasa, S. B.; Zheng, Y.; Shin, Y. K.; Junkermeier, C.; Engel-Herbert, R.; Janik, M. J.; Aktulga, H. M.; Verstraelen, T.; Grama, A.; van Duin, A. C. T. The ReaxFF reactive force-field: development, applications and future directions. *npj Comput. Mater.* **2016**, *2*, 15011.
- (9) Mortier, W. J.; Ghosh, S. K.; Shankar, S. Electronegativity-equalization method for the calculation of atomic charges in molecules. *J. Am. Chem. Soc.* **1986**, *108*, 4315–4320.
- (10) Wood, M. A.; Kittell, D. E.; Yarrington, C. D. Multiscale modeling of shockwave localization in porous energetic material. *Phys. Rev. B: Condens. Matter Mater. Phys.* **2018**, *97*, 014109.
- (11) Zheng, M. *ReaxFF MD Simulation of Coal Pyrolysis Chemical Reaction Based on GPU*; University of Chinese Academy of Sciences: Beijing, 2015.
- (12) Furman, D.; Kosloff, R.; Dubnikova, F.; et al. Decomposition of condensed phase energetic materials: interplay between uni- and bimolecular mechanisms. *J. Am. Chem. Soc.* **2014**, *136*, 4192–4200.
- (13) Strachan, A.; Kober, E. M.; van Duin, A. C. T.; Osgaard, J.; Goddard, W. A. Thermal decomposition of RDX from reactive molecular dynamics. *J. Chem. Phys.* **2005**, *122*, 054502.
- (14) Chenoweth, K.; van Duin, A. C. T.; Goddard, W. A. ReaxFF reactive force field for molecular dynamics simulations of hydrocarbon oxidation. *J. Phys. Chem. A* **2008**, *112*, 1040–1053.
- (15) Chen, Z.; Zhao, P.; Zhao, L.; Sun, W. Molecular Simulation of the Catalytic Cracking of Hexadecane on ZSM-5 Catalysts Based on Reactive Force Field (ReaxFF). *Energy Fuels* **2017**, *31*, 10515–10524.
- (16) Han, S. *Molecular Dynamics Simulation of Initial Reaction between Aviation Kerosene Combustion and Soot Formation*; University of Chinese Academy of Sciences (Institute of Process Engineering, Chinese Academy of Sciences), 2018.
- (17) Nusca, M. J. *Modeling Combustion Chamber Dynamics of Impinging Stream Vortex Engines Fueled with Hydrazine-Alternative Hypergols*; US Army Research Laboratory Aberdeen Proving Ground: MD 21005, 2008.

- (18) William, H. Hypergolic Liquid or Gel Fuel Mixtures. U.S. Patent 20,080,127,551 A1, 2008.
- (19) Dambach, E. M. *Ignition of Advanced Hypergolic Propellants*. AIAA 2010-6984, 2010.
- (20) Pakdehi, S. G.; Shirzadi, B. The effect of some amines on ignition delay time of dimethyl amino ethyl azide (DMAZ) and white fuming nitric acid (WFNA). *Propellants, Explos., Pyrotech.* **2017**, *43*, 162–169.
- (21) Plimpton, S. Fast parallel algorithms for short-range molecular dynamics. *J. Comput. Phys.* **1995**, *117*, 1–19.
- (22) Strachan, A.; van Duin, A. C.; Chakraborty, D.; Dasgupta, S.; Goddard, W. A. Shock waves in high-energy materials: the initial chemical events in nitramine RDX. *Phys. Rev. Lett.* **2003**, *91*, 098301.